OBSERVATIONS OF **MERCURY'S NA-D EMISSION SPECTRUM WITH THE TNG IN AUGUST 2003**

C. Barbieri (1), G. Cremonese (2), S. Verani (1), R. Cosentino (3), F. Leblanc (4), M. Mendillo (5), A. Sprague (6), D. Hunten (6)
(1) Department of Astronomy, University of Padova, Italy, (2) INAF Padova, Italy, (3) INAF TNG, (4) Service de Aeronomie du CNRS, Verrires-Le-Buisson, France, (5) Center for Space Physics, Boston University, USA, (6) Lunar and Planetary Laboratory, Tucson, Arizona, USA

cesare.barbieri@unipd.it

Abstract

The high resolution spectrograph of the 3.5m Galileo telescope (TNG) has been used to obtain several spatially resolved spectra of Mercury's Na-D on the evenings of 8, 9 and 10 August 2003. The resolution was 115000, the slit dimensions were 0".4x27". The paper will present the observations and the will discuss the Na distribution.

Introduction

The existence of the atmosphere around Mercury was discovered by the Mariner 10 spacecraft, which revealed UV emissions of three atomic elements: H, He and O (Broadfoot *et al*., 1976). Three other elements (Na, K, and Ca) were later discovered with ground-based observations (Potter & Morgan 1985, Potter & Morgan 1986, and Bida *et al*. 2000, respectively). Due to the low density (of about $n = 10^5$ atoms/cm^3, $P = 10^{-12}$ bar, on the dayside), the atmosphere is collision-less, i.e., the mean free path of the atoms is longer than the value of the scale height H of the atmosphere (cf. Chamberlain & Hunten, 1987). Therefore, the whole atmosphere is comparable with an exosphere having the exobase coincident with the planet's surface.

To provide more data to help understand the complex phenomena observed in the optical and radar domains, we have undertaken observations of the Na exosphere with the SARG/TNG. The advantages of using the TNG in this context come from the good collecting aperture, from the outstanding image quality of the site and of the telescope, and from the excellent performances of the SARG in terms of efficiency and resolution. The present paper greatly expands on the results obtained in the first, largely exploratory, attempt to reach this goal (Barbieri et. al, 2004, Paper I), and compares the observations with the model of Leblanc and Johnson (2003). We judge the results promising enough to plan a program of observations for the next several years. Not only do we hope to clarify the relative role of source mechanisms but we also hope to provide a useful data bank for the forthcoming space missions MESSENGER and BepiColombo.

Observations and Data Reduction

The SARG has been equipped with a Na filter specifically for this purpose of studying diffuse Na in Solar System objects, because it allows to keep a long slit (26.7 arcsec) on the sky by removing order overlapping. The main characteristics of the spectrograph are given in Table 1.

Table 1 - Instrumentation parameters

Spectrograph resolution	115000
Slit length and width	26.7 x 0.40 arcsec
Pixel dimension and scale	0.022 A, 0.32 arcsec
CCD dimension	2K x 4K pixels

For further information on SARG see http://www.pd.astro.it/sarg/.

The observations discussed here were carried out on three evenings: 8, 9 and 10 Aug 2003 between 19:00 and 20:00 UT, namely during daytime or with the Sun just below the horizon, the minimum elevation of the TNG being 13.5 deg. To save read-out time, the slit was 2x-binned in the spatial direction making the effective spatial pixel of 0.64 arcsec.
The Mercury main parameters were as in Table 2 :

Table 2 – Mercury's parameters

Mercury	8 Aug 2003	9 Aug 2003	10 Aug 2003
Illuminated Fraction	59%		56.2%
Angular Diameter	6.802 arcsec		7.005 arcsec
Mercury-Earth Radial Velocity	0.989 km/s		1.685 Km/s
Mercury-Sun Radial Velocity	**0.462 km/s ???**		-24.690 Km/s
Sun-Earth-Mercury Angle	79.657 deg		82.842 deg

!!!Stefano, complete and check the radial velocities!!!

The 8th and 9th the slit was maintained parallel to Right Ascension (PA = 90°), and placed at several positions across and outside the planet's disk, as in Fig. 1.

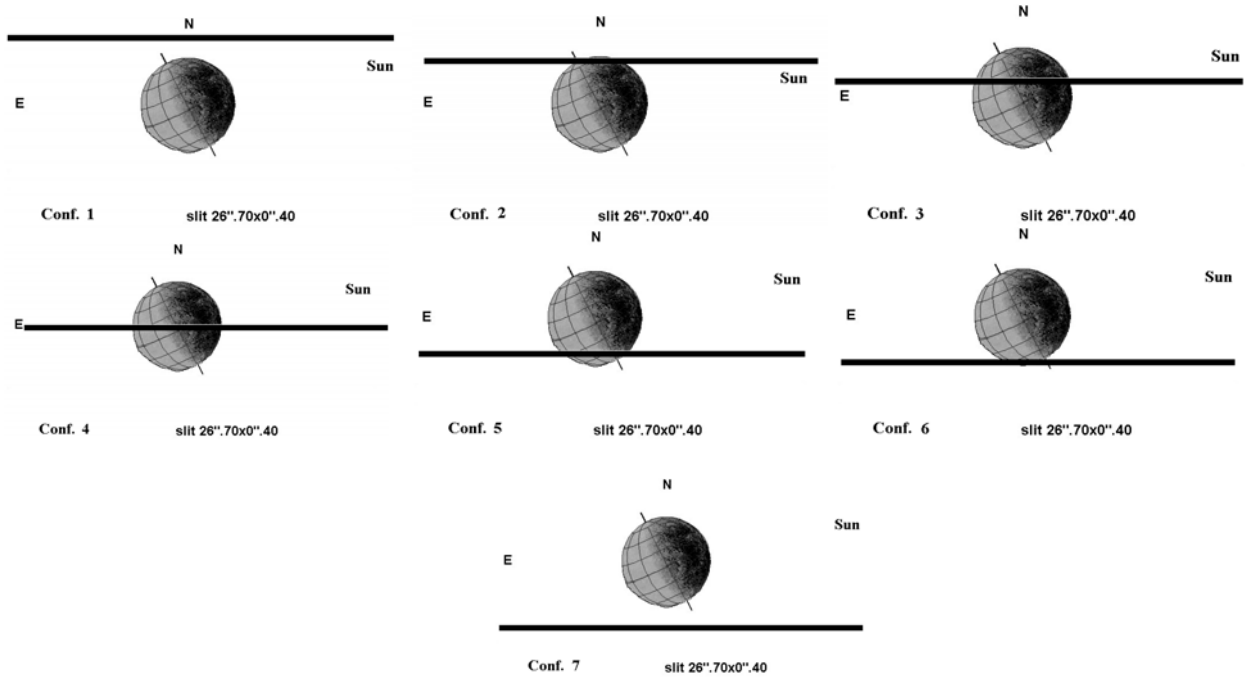

Fig. 1 – The slit configurations for the 8th and 9th Aug 2003

The obtained spectra are detailed in Table 3 and Table 4.

Table 3 – The logbook of the spectra obtained the 8th Aug 2003

Sp Nr.	Exp Time (sec)	Configuration
62	60 sec	Intermediate between 6 and 7
63	60	4
64	60	5
65	60	Intermediate between 6 and 7
66	60	1
67	60	Intermediate between 2 and 3
68	60	4
69	60	5
70	Uncertain (telescope hits limiting switch)	6

Table 4 - The logbook of the spectra obtained the 9th Aug 2003

Sp Nr.	Exp Time (sec)	Configuration
15	60	4
16	90	4
17	90	7
18	90	6
19	90	5
20	90	4
21	90	Intermediate between 1 and 2
22	90	1
23	90	1
24	90	2
25	90	3
26	90	4
27	90	Intermediate between 5 and 6
28	90	7
29	90	7+
30	10 ? Uncertain, telescope hits limiting switch	4

The 10th, the slit was instead placed along the Declination (PA = 0°), and the observed configurations are as in Fig. 2.

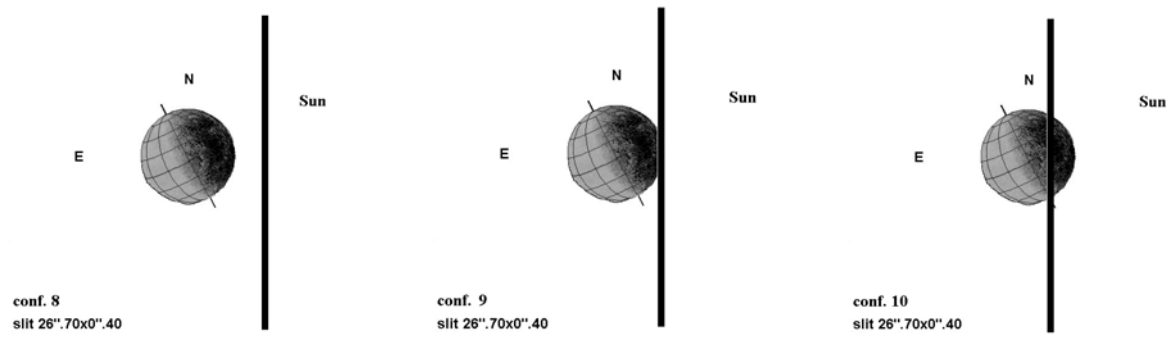

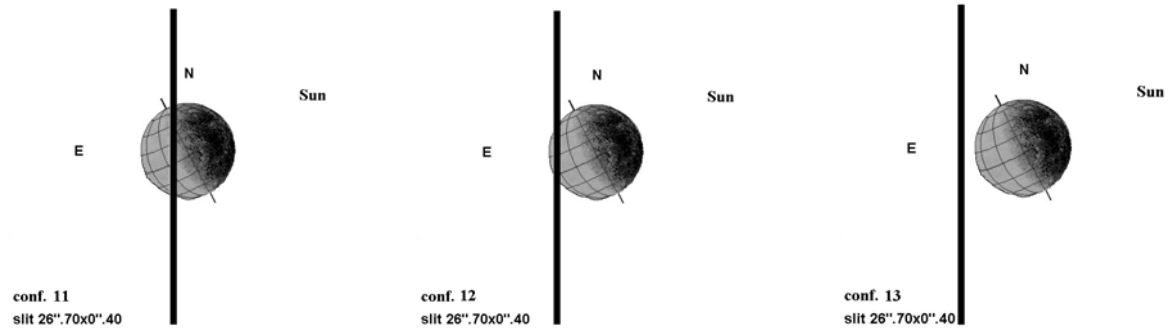

Fig. 2 – The slit configurations for the 10th Aug 2003.

The obtained spectra are shown in Table 5.

Table 5 – The logbook of the spectra obtained the 10th Aug 2003

Sp Nr.	Exp Time (sec)	Configuration
35	30	8
36	60	8
37	60	Intermediate between 9 and 10
38	60	Intermediate between 10 and 11
39	60	13
40	60	Intermediate between 10 and 11
41	60	8
42	90	8
43	90	9
44	90	Intermediate between 10and 11
45	90	Intermediate between 11and 12
	90	13

Examples of the spectra are shown in Fig. 3.

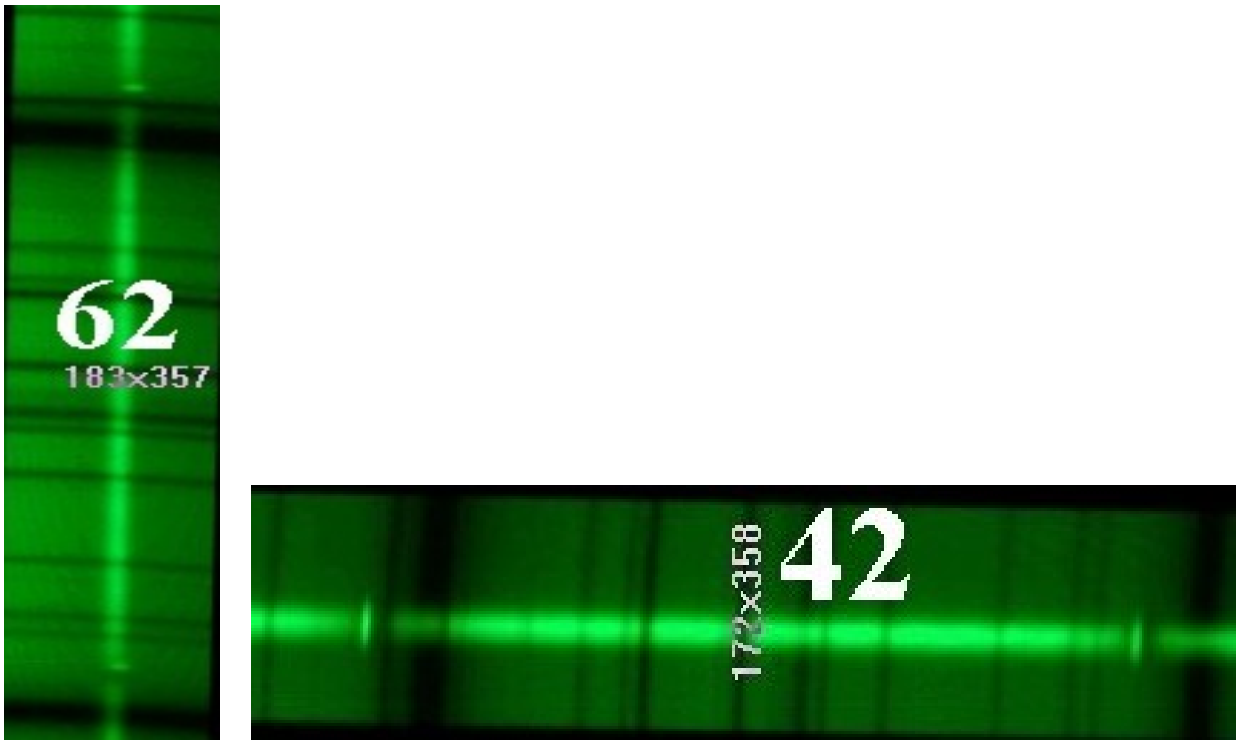

Fig. 3 – Examples of raw spectra obtained with the slit in PA 90° (slit E-W) and PA = 0° (slit N-S) respectively. The long slit permits an accurate subtraction of the night sky continuum. The disk of the planet is spatially resolved, with a seeing PSG varying from 1".2 to 1".8.

The stars Alfa Vir (Spica), Beta Leo (Denebola), and 61 Uma were observed as reference for Point Spread Function and for flux calibration, as explained in Paper I.

Calibration of the Spectra

Fig. 4 shows the traces of instrumental data numbers (ADU) along the slit for the continuum, and for the D2 and D1 lines. The conversion to column abundance was performed with a method due to Sprague *et al.* (1986) and Sprague *et al.* (1997). The parameter RR derives from the Hapke rough-reflectance surface model (Hapke 1986) at each location in the surface grid. The grid-size can be chosen to represent the parameters of the spectrograph (in this case a spatial pixel of 0.32 arcsec binned x 2, namely 0.64 arcsec). The Hapke RR can then be used to absolutely calibrate the data using an average of the maximum values from the continuum at a wavelength close to the sodium D lines. The result is shown in Table 6. The axis *x* is on the planet equator, positive toward East. The continuum brightness is expressed in MRayleigh/Angstrom, the D2 and D1 in KRayleigh.

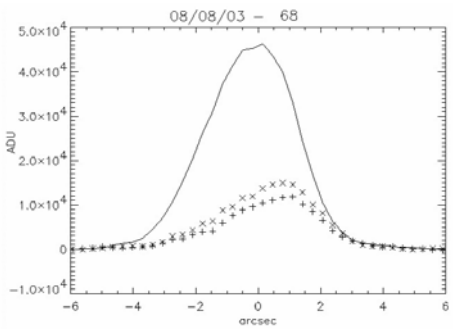

Fig. 4 – The tracing of spectrum nr. 68. Thick Line: continuum; crosses x = D2; plus + = D1

Table 6 – The calibration of Sp. 68

Distance x (arcsec)	Distance y (arcsec)	Continuum (counts)	RR factor	Mercury Brightness (MR/A)	D1 (KR)	D2 (KR)	Column Abundance (E13)
-0,92	-0,43	1083,23	*3,23*	***0,99***	**347,6**	**361,5**	**0,051**
-0,63	-0,29	2219,16	*6,68*	***2,04***	**435,4**	**561,4**	**0,088**
-0,34	-0,16	3596,79	*10,85*	***3,31***	**809,7**	**982,6**	**0,362**
-0,05	-0,02	5760,49	*17,38*	***5,31***	**1286,1**	**1773,3**	**0,873**
0,24	0,11	8781,30	*26,08*	***8,58***	**1395,9**	**1987,9**	**0,866**
0,53	0,25	12207,63	*37,24*	***11,68***	**1988,8**	**2655,6**	**1,676**
0,82	0,38	15807,15	*47,06*	***14,37***	**2405,5**	**3535,7**	**2,096**
1,11	0,52	18561,55	*58,09*	***17,74***	**2586,6**	**4004,3**	**2,252**
1,40	0,66	21468,42	*66,82*	***20,41***	**3570,1**	**5546,2**	**4,035**
1,69	0,79	24420,76	*73,24*	***22,37***	**4654,3**	**5803,6**	**5,903**
1,98	0,93	26426,73	*78,79*	***24,06***	**5320,8**	**6972,0**	**6,945**
2,27	1,06	27390,79	*82,74*	***25,27***	**5872,3**	**7285,8**	**6,161**
2,56	1,20	27362,68	*83,48*	***25,49***	**6463,7**	**8474,7**	**7,171**
2,85	1,33	25639,49	*79,65*	***24,32***	**6976,0**	**9140,0**	**7,753**
3,14	1,47	23640,68	*73,42*	***22,92***	**7343,4**	**9399,5**	**7,934**
3,43	1,60	19253,04	*59,69*	***18,23***	**7420,4**	**9176,1**	**7,497**
3,72	1,74	14146,92	*43,08*	***13,16***	**6243,5**	**7960,6**	**5,102**
4,01	1,87	9493,28	*28,35*	***8,66***	**5201,8**	**6176,1**	**3,167**
4,30	2,01	5875,42	*13,46*	***5,48***	**4011,9**	**4999,9**	**1,839**
4,59	2,14	3699,84	*11,09*	***3,39***	**2523,0**	**3288,8**	**0,657**
4,88	2,28	2165,06	*6,41*	***1,96***	**1693,5**	**2162,3**	**0,249**
5,17	2,41	1189,77	*3,61*	***1,10***	**1066,2**	**1162,0**	**0,073**

Comparison with Leblanc and Johnson (2003) model

We adapted the model described in Leblanc and Johnson (2003) and Leblanc et al. (2003) for the same heliocentric positions and geometry of the observations (phase angle, ecliptic inclination of Mercury's axis and seeing effects). No change was made in the parameters of the simulation already described in these papers (same meteoroid flux, same parameter for the solar wind and solar photon flux, same surface temperature...).

In all the comparison between observations and simulation and for all the nights we estimated the best slit positions within the uncertainty given by the observations (as an example, when the observations refer to a position intermediate between configuration 5 and 6, the uncertainty is roughly 0.5"). In the Figures, the negative distance along the slit corresponds to the anti sunward direction in the case of 8th and 9th Aug 2003, and to South direction in the case of the 10th Aug 2003.

The value for the seeing which is crucial in this comparison is based on star observations during the same nights. Such observations indicate values of 1.6, 1.7 and 1.2" for the seeing during the 08/08/2003, 08/09/2003 and 08/10/2003 respectively. It is however true that the stars were observed at zenith angles much higher than Mercury's (close to the sun and therefore at low zenith angle). Therefore, it is expected that such values should be increased for Mercury's observations. We will discuss the potential effect of this parameter on our results, in particular for the last night. In our simulation, we used for each night the value of the seeing indicated in the caption of Fig. 5, Fig. 6 and Fig. 7.

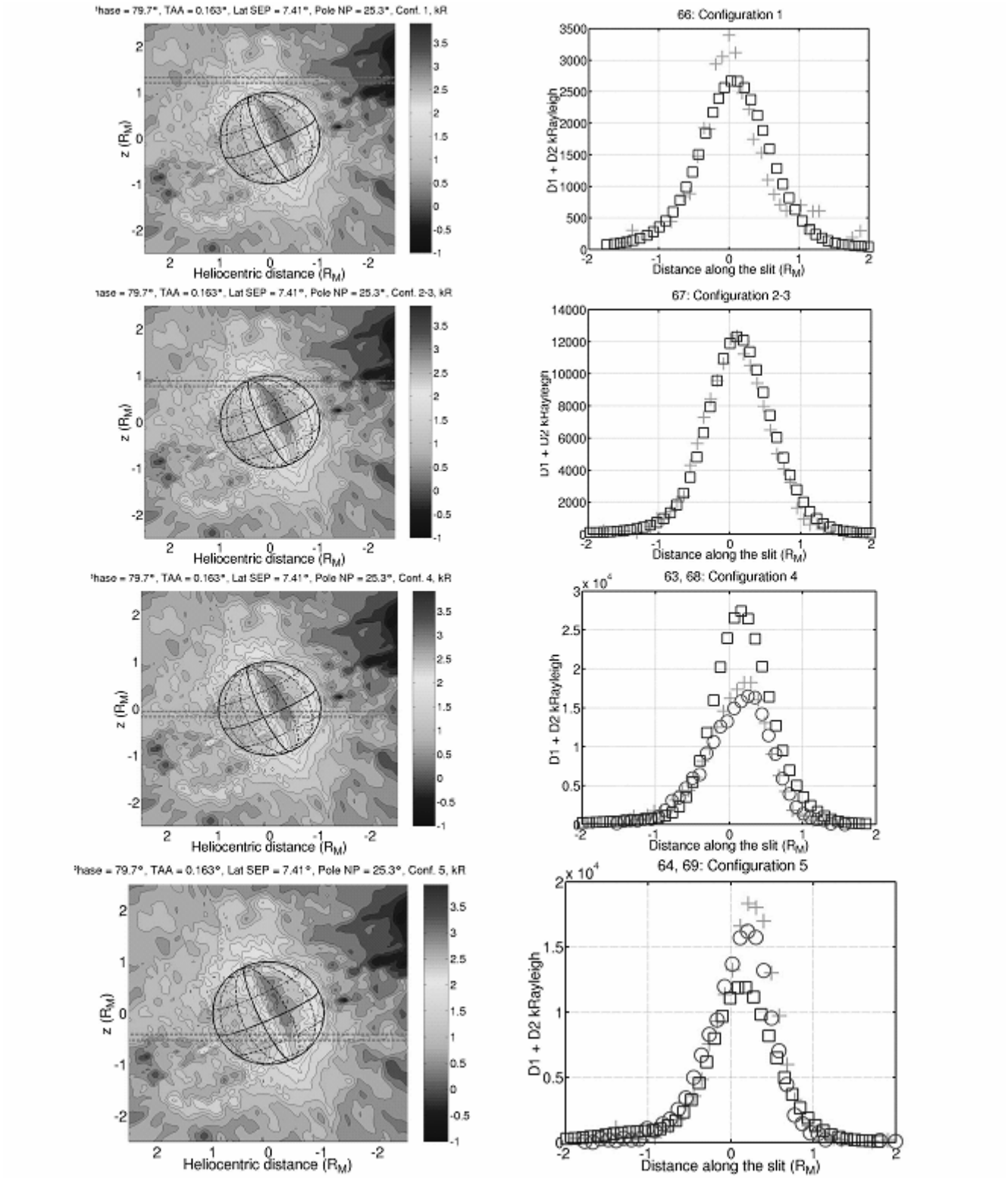

Fig. 5 - First night: 8 Aug 2003, adopted seeing 1.4". First column: Rayleigh emission of the D1+D2 lines calculated by the simulation (Log10). Second column: simulation (blue squares) and observations (green crosses).

For the night 08/08/2003, the comparison between model and observations is good for slit positions in the Northern hemisphere both in term in intensity and shape of the emission. Let us remark however that the intensity of the simulated signal depends also on the seeing value. A larger seeing value implies a larger peak of emission. The seeing value has been estimated as the best value for both shape of the emission and peak of the intensity. In the Southern hemisphere the agreement is poorer, indicating that the

!!! Francois, check ‘measured emission is larger than observed’. Explain the red dots. His ‘Heliocentric’ the right caption???

The contrary situation is suggested at the equator. It seems therefore that the distribution of the exospheric material is different from the simulation, with a smaller source at the equator and a larger source in the Southern hemisphere. However, as explained in the introduction, in configuration 6-7 (for example) a slit position slightly different than supposed here could change significantly the result.

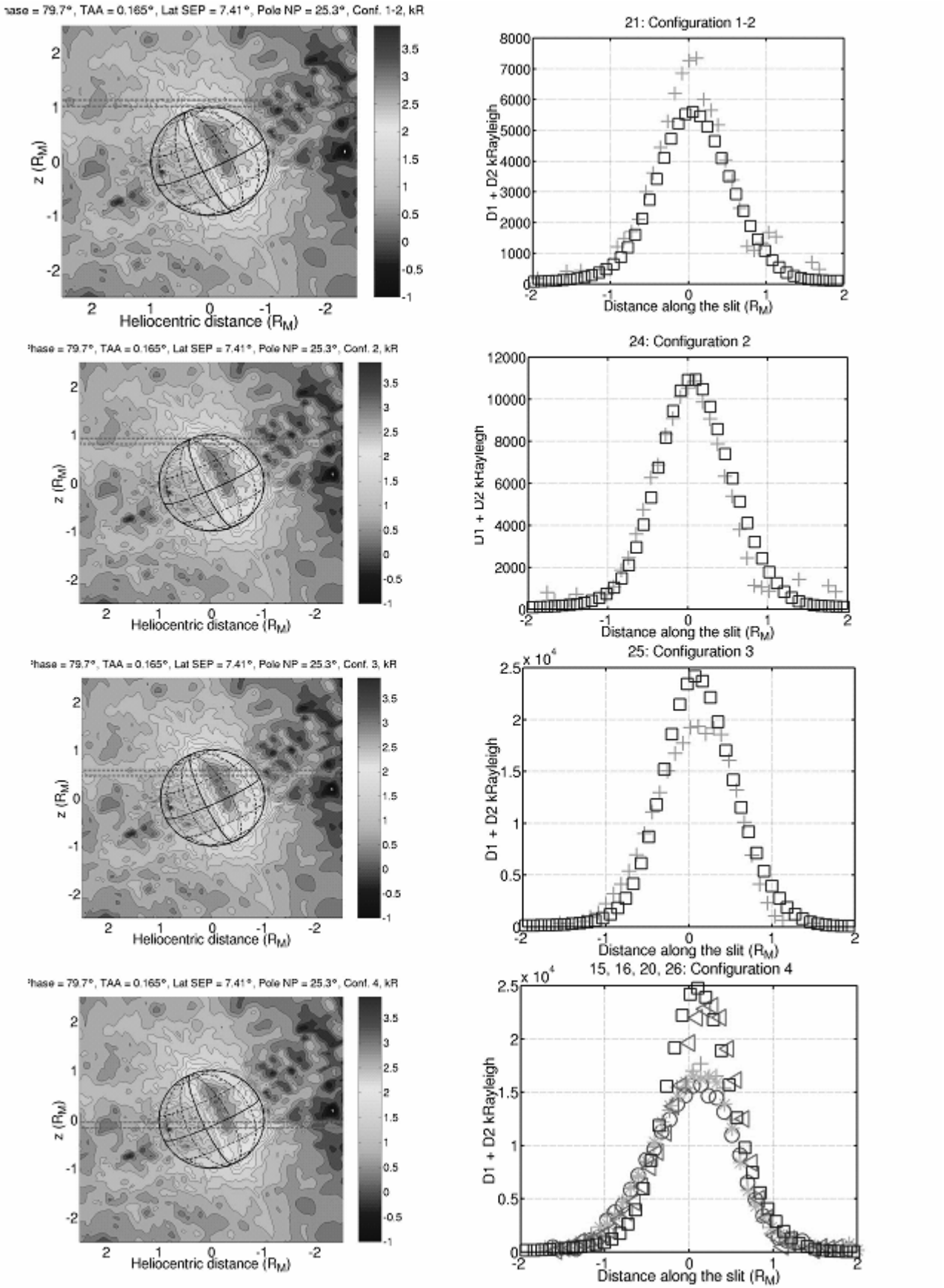

Fig. 6 - Second night of observations: 9 Aug 2003, adopted seeing 1.5". First column: Rayleigh emission of the D1+D2 lines calculated by the simulation (Log10). Second column: simulation (blue squares) and observations (green crosses).

The agreement between observations and simulation is here better than the previous night. It is first of all very interesting to remark that the general size of intensity is in good agreement with the simulation, which confirms that the size

!!!Francois, what do you mean by size??

and distribution of the sodium exosphere simulated by our model provide a satisfying solution for the observations. However, the same North - South discrepancy is also observed here, with the simulation signal smaller than the measured one in the South. The configuration 7 illustrates how two supposedly similar positions of the slit can correspond to very different emissions when such position is close to the limit of the exospheric cloud. Configuration 4 is here also indicative of the potential variation of the emission within 30 minutes of observations, either due to the uncertainty on the exact position of the slit or to intrinsic variation of the emission.

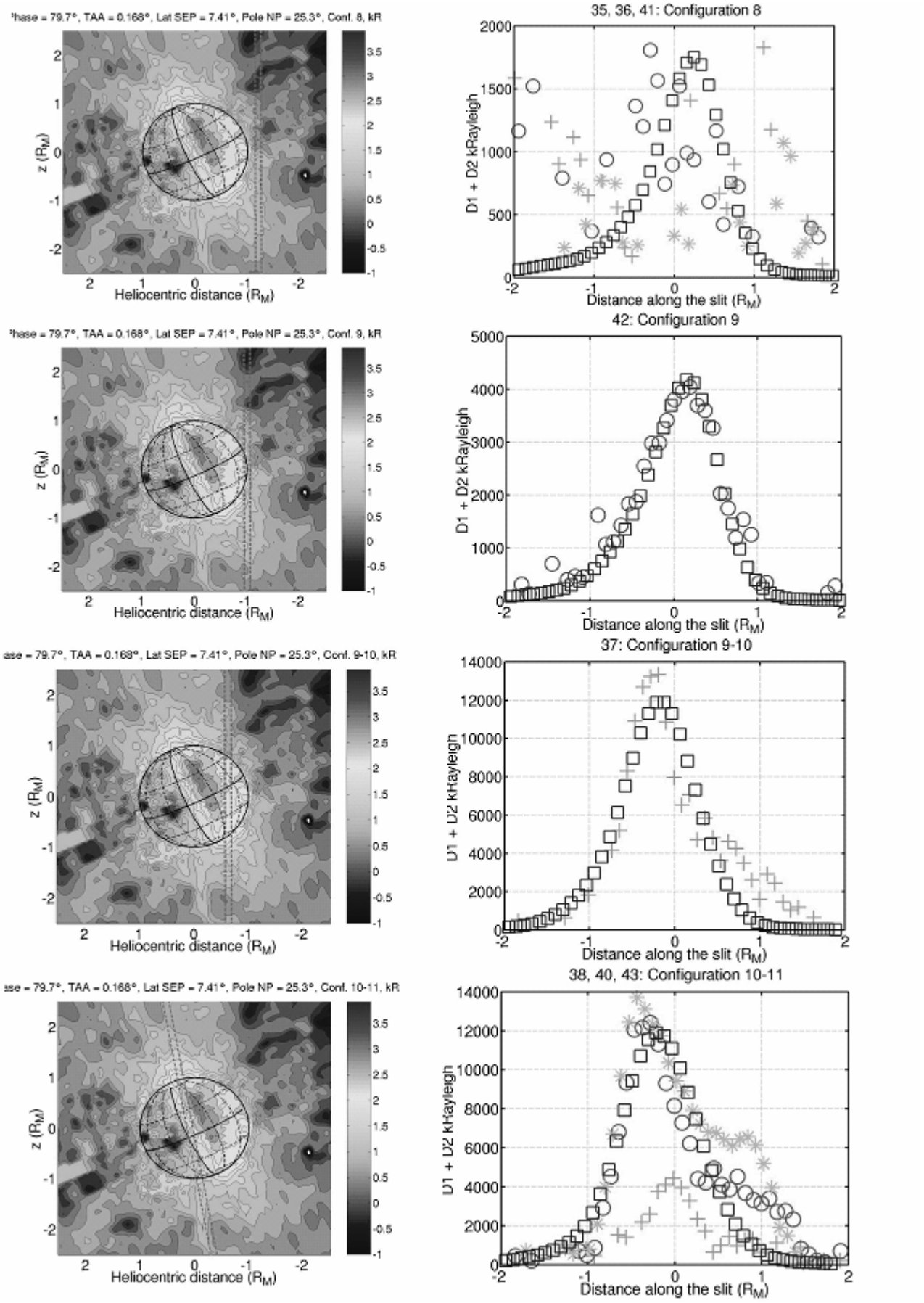

Fig. 7 - Third night of observation 10 Aug 2003, Seeing used 1.2". First column: Rayleigh emission of the D1+D2 lines calculated by the simulation (Log10). Second column: normalized simulation (blue squares) and observations (green crosses).

For the Aug. 10 observations, the agreement is also good in term of intensity but it is not as good as the previous nights for the shape of the emission. A difficulty inherent to this slit configuration is the precise position of the slit itself. Indeed, a small uncertainty on the orientation of the slit with respect to the North-South and East-West directions can have significant difference in the observed signal. The slit orientation was allowed to be slightly tilted with respect to the North-South axis in order to better fit the data (see first column of Fig. 7), by +10° for configuration 10-11 and by -5° for configuration 11-12. For the other configurations we did not include any tilt of the slit. Such tilt in the case of configuration 10-11 improves the agreement between the rapid increase of the emission in the negative distance range, and for configuration 11-12 it improves the agreement at the maximum of the intensity. The second conclusion that can be made from Fig. 7 is the presence of a second peak of sodium in the exosphere placed at positive distance along the slit (particularly apparent in configuration 9-10 and 10-11). In Fig. 8, we show the result of a further comparison in which we include *arbitrarily* a second peak of emission above the North pole of Mercury and outside of the disk. We adjusted this second peak in order to get the best agreement between observations and simulation (intensity, position and variation). In reality, we also defined this second peak in order to roughly correspond to a strong source of sodium on the late afternoon side (that is behind the disk for the observer).

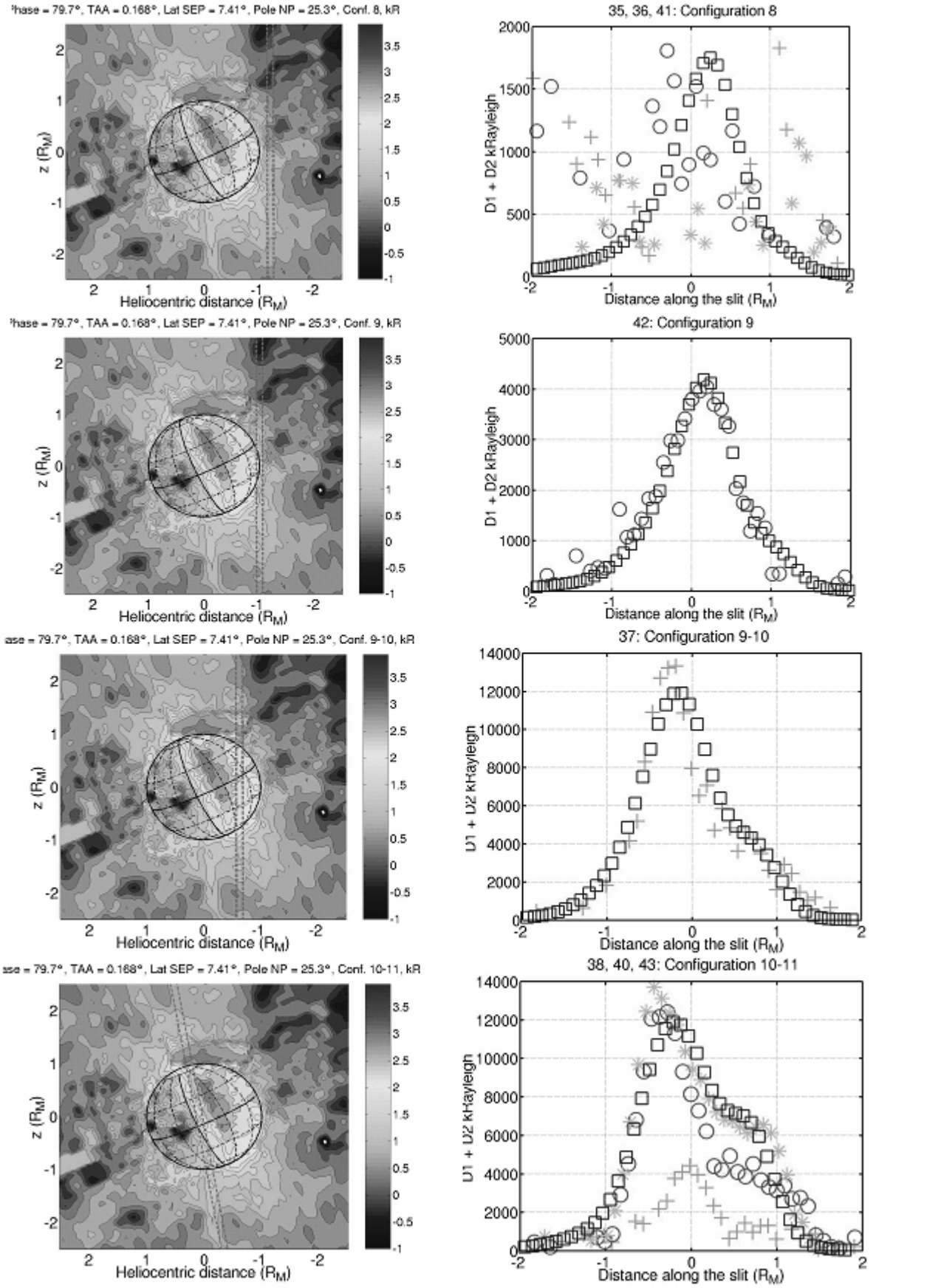

Fig. 8 - Third night of observation 10 Aug 2003, with an added emission above the North pole in order to get the best agreement.

The agreement is significantly improved for configurations 9, 9-10 and 10-11. It indicates that a second important source could be at the origin of the particular shape of the emission observed during this night (something that is not seen during the two previous nights). The agreement is not improved for configuration 13 (which in any case corresponds to a very noisy emission), and is decreased for configuration 11-12. However, such last observation is problematic for several reasons, the measured intensity is almost as large as for a slit placed on the dayside (configuration 11-12 corresponds to a slit entirely on the night side), and the width of the measured emission along the slit cannot be reproduced with the seeing supposed in this observation (that is 1.2"), it could be reproduced only with much smaller value. We will perform further simulations to model what could be the origin of such emission.

Conclusions

It has been confirmed that the SARG/TNG can provide significant data for Mercury's Na exosphere.
Our simulation seems to reproduce several observed characteristics (intensity of the emission, shape of the emission along each slit). Some discrepancies remain which suggest:
- a stronger source of sodium in the North and South high latitudes of Mercury (a stronger redistribution of the Na at its surface?),
- some short time variation of the emission (from one night to another), here due to a source of exospheric sodium from the late afternoon .

References

Barbieri C., Verani S., Cremonese G, Sprague A., Mendillo M., Cosentino R., Hunten D., 2004, Planetary and Space Sciences, in press (Paper I)

Hapke, B., Bidirectional reflectance spectroscopy: 4. *The extinction coefficient and the opposition effect*. **Icarus**, 67: 264 – 280, 1986

Leblanc, F. and Johnson, R.E., *Mercury's sodium exosphere*. **Icarus**, 164(2): 261-281, 2003.

Sprague A.L., Kozlowski R.W.H., Hunten D.M., Schneider N.M., Domingue D.L., Wells W.K., Schmitt W., Fink U., *Distribution and Abundance of Sodium in Mercury's Atmosphere*, 1985-1988, **Icarus 129**, 506-527, 1997.